

Influence of silicon, strontium and aluminum oxides on silicon nitride ceramics for bone replacements

Sergio Ferreira do Nascimento¹, Andrea Cecilia Dorion Rodas²,
Flávio Machado de Souza Carvalho³, Olga Zazuco Higa¹,
Cecilia Chaves Guedes e Silva¹

¹ Instituto de Pesquisas Energéticas e Nucleares, Avenida Professor Lineu Prestes 2242, São Paulo, SP, Brazil.

² Centro de Engenharia, Modelagem e Ciências Sociais Aplicadas, Universidade Federal do ABC, Alameda da Universidade s/nº, São Bernardo do Campo, SP, Brazil.

³ Universidade de São Paulo, Rua do Lago 562, São Paulo, SP, Brazil.

e-mail: sergiofnasc@gmail.com

ABSTRACT

Although silicon nitride ceramics have been shown very propitious to be used for bone replacements, some characteristics can be controlled to improve their osseointegrations process. One of them is the intergranular phase whose composition can be specified to stimulate mineralization and osteoblastic production. In this paper, the intergranular glassy phase was projected in order to contain silicon, strontium and aluminum oxides. Silicon nitride samples containing different contents of SiO₂, SrO and Al₂O₃ were sintered at 1815°C for 1 hour and characterized by scanning electron microscopy and X-ray diffraction. Hardness and fracture toughness were determined by Vickers hardness test and compressive strength was evaluated using an universal material testing machine. The biological behavior was studied in regard to cytotoxicity and cell proliferation by means of *in vitro* experiments. The samples reached high densities (higher than 95 %TD), total $\alpha \rightarrow \beta$ -Si₃N₄ transformation, fracture toughness higher than 6.5 MPa.m^{1/2}, compressive strength up to 2500 MPa and Vickers hardness less than 9.8 GPa. All samples were non-cytotoxic and able to promote cell proliferation with great potential to be used as components for bone replacements. However, that sample with high content of strontium had the best results of cell proliferation, proving the importance of a careful choice of intergranular phase composition in silicon nitride ceramics.

Keywords: silicon nitride, mechanical properties, osteoblasts.

1. INTRODUCTION

Silicon nitride (Si₃N₄) is a ceramic material widely used in structural applications whose properties depend on porosity, grains morphology and secondary phases present in the microstructure [1-3]. Many recent researches have focused on the performance of silicon nitride as biomaterial [4, 5]. KERSTEN *et al.*, [6] for example, implanted silicon nitride and PEEK (polyetheretherketone) cages into lumbar spines of Dutch milk goats and observed higher fusion rates for silicon nitride than PEEK. Other study using peripheral blood mononuclear cells (PBMNCs) compared silicon nitride particles with cobalt-chromium and Ti-6Al-4V alloys and showed that silicon nitride promoted a minimal impact in PBMNCs [7]. In addition, the bacteriostatic properties of silicon nitride have also been evaluated. A study of BOCK *et al.* [8] about the bacterial (*S. epidermidis* and *E. Coli*) attachment and proliferation on PEEK, Ti-alloy and Si₃N₄ demonstrated that Si₃N₄ can inhibit the biofilm formation. BOSCHETTO *et al.* [9] observed the same positive effect concluding that surface chemistry of silicon nitride can hinder biofilm formation and bacterial proliferation.

Investigations about the porous and dense silicon nitride ceramics obtained by different processing techniques and parameters as well as space holders and sintering aids have also been carried out [10-14]. These researches indicate that a good way to improve the biocompatibility of silicon nitride ceramics is carefully selecting their sintering additives. An appropriate selection of additives may promote the liquid sintering of silicon nitride and obtaining of components with adequate mechanical properties and *in vivo* reactivity. As it is known [15, 16], the sintering additives should react with the silica layer presents on silicon nitride powder surface to form a liquid phase at the sintering temperature, so that the α -Si₃N₄ phase is dissolved and reprecipitated in the β -Si₃N₄ phase. After cooling step, the liquid phase remains in the grain boundaries of silicon nitride as a crystalline or amorphous secondary phase which tends to influence the final properties of

the material.

The most commonly compounds used as silicon nitride sintering aids are the rare earth oxides. Rare earth oxides may promote the liquid sintering of silicon nitride by means of a viscous liquid which favors the development of elongated β - Si_3N_4 grains. Moreover, the liquid phase can crystallize during the cooling process or after specific heat treatments, producing materials with improved thermo-mechanical properties to be used in structural application in aggressive environment [17, 18].

Although some studies have shown that silicon nitride ceramics doped with Y_2O_3 , Yb_2O_3 and Al_2O_3 [12, 19, 20] are suitable for biomedical applications, other ones have shown that additives such as SiO_2 , CaO , Bioglass and hydroxyapatite [10, 13, 21] can promote the formation of bioactive secondary phase, accelerating the osseointegration process.

This paper evaluates the effect of additions SiO_2 , SrO and Al_2O_3 in the densification, microstructure, mechanical properties and *in vitro* cytocompatibility of silicon nitride ceramics to be used in maxillofacial surgery, mini-osteofixation systems, intervertebral fusion spacers and dental roots [22]. The additives combination was choose based on the previous studies results that showed the potential of silica and alumina to promote efficient liquid sintering of silicon nitride and to produce components with good mechanical properties and excellent *in vitro* biological behavior [21]. The proposed compositions should increase the bone-implant interaction owing to silica addition, as well as to promote the osteoblasts proliferation as a result of strontium release into the patient, increasing the potential of the sintered material for biomedical applications [23].

2. MATERIALS AND METHODS

2.1 Samples preparation

The raw materials used for the present study were: α - Si_3N_4 powders (UBE, SN-E10), SiO_2 (quartz, 99.9% purity, Sigma-Aldrich), Al_2O_3 (99.9% purity, Almatris, CT 3000SG) and SrCO_3 (98% purity, Sigma-Aldrich).

Six compositions containing different contents of the described raw materials were investigated according Table 1. Powder mixtures with proper proportions were ground in a ball milling for 24 hours using isopropanol as liquid media. After drying in a rotary evaporator, powders were uniaxially pressed at 50 MPa followed by cold isostatic pressing (200 MPa), to form pellets. The green compacts were embedded in a Si_3N_4 powder bed in a BN coated graphite crucible and sintered in graphite resistance furnace (Thermal Technology) in a high purity nitrogen atmosphere. After sintering, all samples were rectified using a diamond wheel.

Table 1: The selected compositions (wt.%)

COMPOSITION	Si_3N_4	SiO_2	SrO	Al_2O_3
Se6	90	6	4	0
Se6a	90	6	3.86	0.15
Se10	80	10	10	0
Se10a	80	10	9.625	0.375
Se12	80	12	8	0
Se12a	80	12	7.7	0.3

2.2 Density, Porosity and Microstructure Analysis

Apparent density and porosity were measured using the Archimedes' principle. While the relative density was determined considering the theoretical densities of each composition, calculated by the rule of mixtures.

In order to investigate the samples microstructure, polished and plasma-etched (using SF_6/O_2 gas mixtures) samples surfaces were analyzed by scanning electron microscopy (Philips - XL30 microscope). The crystalline phases were determined by X-ray diffraction (XRD) using a Brucker D8 X-ray diffractometer with $\text{Cu K}\alpha$ radiation and a scanning step of 0.02. Scans were obtained from 5° to 10° at 2° per minute.

2.3 Mechanical Properties

The Vickers hardness were investigated using a hardness tester (Buhler VH1150 Durometer) and a load of 100 N with loading time of 15 s at room temperature. Seven indentations were carried out in each sample and the hardness values were calculated by Equation (1), in which Hv is Vickers hardness, P is applied load, and d is the average value of the measured diagonals.

$$Hv = \frac{1,8544 \times P}{a^2} \quad (1)$$

The values of indentation fracture toughness (K_{Ic}) were obtained evaluating the same impressions obtained by the Vickers hardness test and using the equation of ANSTIS *et al* [24]. The compressive tests of ten samples of each composition, with dimensions of approximately 5.60 mm diameter and 3.00 mm in thickness, were conducted with loading speed of 4.0 mm/min using an universal material testing machine (Instron 4400).

2.4 In vitro Cytotoxicity

In vitro cytotoxicity tests were performed by indirect method according to ISO 10993- standard. Therefore, samples extracts (final concentration of 6 cm²/mL) were prepared incubating sterilized silicon nitride samples into Dulbecco's Modified Eagle Medium (DMEM, Gibco) with 10% fetal bovine serum (FBS) at 37° C for 72 h.

At the same time, 3T3-NIH cells (mouse fibroblasts, ATCC) were seeded (2×10^4 cells/well) and incubated during 24 h in Minimum Essential Medium (MEM, Gibco) with 10% FBS, at 37 °C in 5 % CO₂. After, the medium was replaced by the extracts and the plates were incubated for 24 h at 37 °C in 5 % CO₂. The extracts were exchanged by culture medium containing MTS vital dye (Promega), which reacts with living cells to form a colored compound. Lastly, the absorbance of the culture medium + MTS was measured by an Elisa Plate Reader (wavelength of 490 nm) and the cell viability was calculated according Equation 2.

$$cell\ viability = \frac{OD_{sample}}{OD_{control}} \times 100 \quad (2)$$

Where OD_{sample} is the optical density of the sample and $OD_{control}$ is the optical density of the control (aliquots of the sterile media).

2.5 Cell Proliferation

Human osteoblast-like cells (MG63, ATCC) were cultured in Minimum Essential Medium Medium (Gibco) supplemented with 10 % fetal bovine serum (Cultilab) and 1 % antibiotic/antimycotic solution (Gibco) at 37 °C in humidified atmosphere containing 5% carbon dioxide. The culture media was changed every 3 days until the confluence of the cultures which were placed in plates, after washing with PBD (phosphate-buffered saline) and trypsinization (0.05 %-EDTA 0.02 % solution at 37 °C for 5 min). Therefore, sterilized silicon nitride samples were placed in 24-well culture plates and 2×10^4 cells/sample were added and incubated at 37 °C. The culture medium was changed every 3 days.

MG63 cells proliferation and viability were investigated in samples subjected to 7 and 21 days of culture by MTS assay. The MTS (Promega) reagent was added to culture medium containing the samples and the cells, standardized as 500 µL for each sample. After 2 h incubation, supernatant aliquots were transferred to a 96-well plate and the absorbances at 492 nm read using an Elisa Plate Reader.

The samples with attached cells were dehydrated and fixed in formaldehyde in order to analyze cells morphology by scanning electron microscopy (SEM, Philips-XL30 microscope).

3. RESULTS AND DISCUSSION

The porosity and density results of the sintered samples with different compositions are shown in Table 2. The high values of relative density, between 95 and 98 %TD, make evident that silicon, strontium and aluminum oxides are very efficient as sintering aids of silicon nitride ceramics, also considering the selected amounts in all studied compositions. It is also clear that the higher total amounts of additives conducted to substantial improvements in material densification (higher density and lower porosity), as we can see comparing the results of Se6 and Se12 coded samples as well as those of Se6A and Se12a, which have the same type and proportion of additives but the Se12 and Se12A with higher total amount (20 % wt.).

Still evaluating the data in Table 2 and comparing the density results of the samples with the same total amounts of additives but with purposefully different mass ratio of SiO₂ to SrO, i.e., Se10 versus Se12 and

Se10a versus Se12a, it is possible to verify the positive effect of the high content of strontium oxide which led to a slight improved densification in the Se10 and Se10A samples. On the other hand, no significant contribution was found due to the presence of low alumina contents in Se6A, Se10A and Se12A samples.

The good performance of both kind and amount of sintering aids are proved when we analyzed the results related by other studies. For example, MATOVIC *et al.* [25] obtained silicon nitride ceramics with Li_2O_3 and Y_2O_3 as additives reaching relative densities ranging from 83.8 to 98 %. WHILE DAS *et al.* [26] obtained samples with a density of 93 %, using the typical combination of Al_2O_3 and Y_2O_3 .

By Figure 1, it is possible to note that the X-ray diffraction results of the sintered samples are in good agreement with those of density shown in Table 2, since all selected compositions reached total $\alpha \rightarrow \beta$ transformation, pointing to the success of additives combination and sintering conditions. In other words, the oxides used as sintering aids formed a liquid phase during the sintering temperature with appropriated characteristics to make feasible the liquid sintering process. The absence of other crystalline phases in the diffractograms, except in that of Se12A sample, demonstrates that the liquid phase formed during sintering remained in the grain boundaries and triple points of silicon nitride grains as an amorphous secondary phase, after cooling step. This kind of microstructure, characterized by $\beta\text{-Si}_3\text{N}_4$ grains involved by a glassy phase rich in silica and strontium, is very promising for bone replacements to combine the great mechanical properties of $\beta\text{-Si}_3\text{N}_4$ phase with the potential bioactivity of the silica-rich glass containing Sr cations, which have been shown to stimulate the *in vivo* osteoblasts proliferation. Besides, the Si_2ON_2 phase found in sample Se12A should not deteriorate the properties of the final material, considering its morphological similarity to $\beta\text{-Si}_3\text{N}_4$ phase.

Table 2: Apparent porosity (P), apparent density (ρ) and relative density (RD) of the silicon nitride samples.

COMPOSITION	P (%)	ρ (g/cm ³)	RD (% TD)
Se6	0.68 ± 0.01	2.99 ± 0.04	95.12 ± 0.36
Se6a	0.43 ± 0.13	3.00 ± 0.05	95.33 ± 0.48
Se10	0.41 ± 0.11	3.12 ± 0.02	98.86 ± 0.43
Se10a	0.43 ± 0.15	3.11 ± 0.02	98.73 ± 0.36
Se12	0.42 ± 0.18	3.05 ± 0.01	98.18 ± 0.46
Se12a	0.46 ± 0.14	3.05 ± 0.01	98.14 ± 0.33

In fact, when observing the microstructure of the polished and etched samples surfaces in Figure 2, we found no difference in the grain morphology developed by the Se12A sample compared to others. Despite this, all samples present a microstructure with elongated $\beta\text{-Si}_3\text{N}_4$ involved by the secondary glassy phase, as also reached by other studies, such that of LIU *et al.* [27] whose samples presented an interlocking microstructure of $\beta\text{-Si}_3\text{N}_4$ grains with high aspect ratio.

However, it is possible to verify that both Se6 and Se6A coded samples are formed by grains of $\beta\text{-Si}_3\text{N}_4$ smaller than the others. As these samples have lower amount of additives in their compositions, this fact must be associated to the lower amount of liquid phase formed during the sintering temperature, which probably favored the precipitation of higher concentration of $\beta\text{-Si}_3\text{N}_4$ nuclei what limited the crystalline growth.

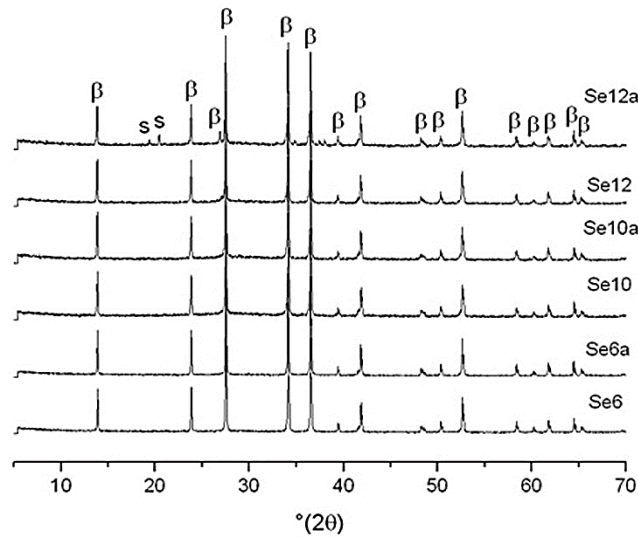


Figure 1: X-ray powder diffraction of the sintered samples (β is β -Si₃N₄ and s is Si₂ON₂).

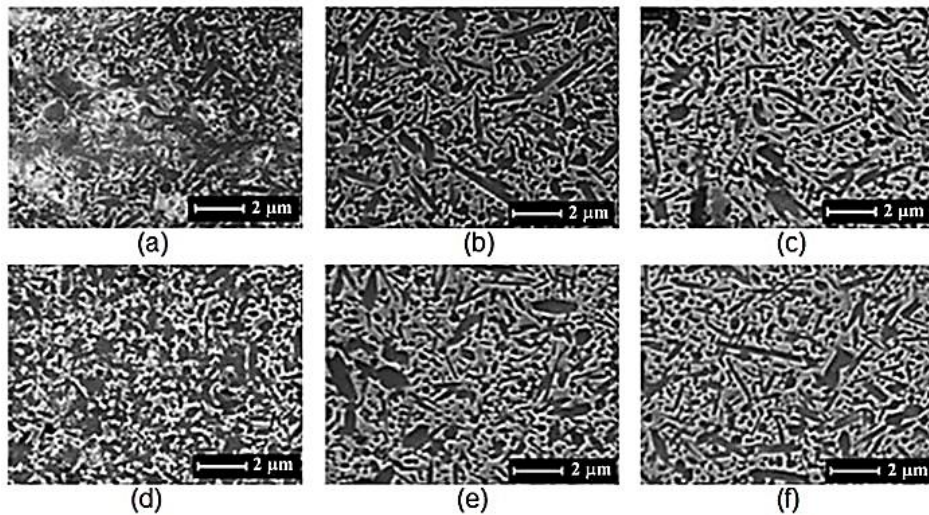


Figure 2: Images of scanning electron microscopy of polished and etched samples surfaces. (a) Se6; (b) Se10; (c) Se12. (d) Se6A; (e) Se10A; (f) Se12A.

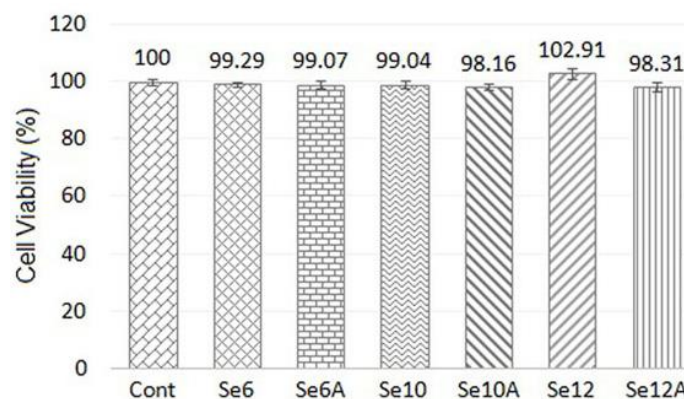
Table 3 shows the results of mechanical properties of the materials. No significant difference is observed in values of fracture toughness and compressive strength among the six compositions. However, these values can be considered well suitable for the proposed applications, i.e., joint components, intervertebral spacers and other orthopedic and dental prostheses, mainly when we consider other studies with different sintering aids of silicon nitride ceramics [15, 17].

The values of hardness tended to be reduced due to the presence of alumina (see Se6 versus Se6A; Se10 versus Se10A and Se12 versus Se12A) and the high content of additives which promoted the formation of higher volume of vitreous phase, softer than β -Si₃N₄ phase. Besides other studies related in the literature, our results of hardness were considerably low. Even in the work of LIU *et al.* [27] that used silica, magnesia and alumina as sintering aids, dense silicon nitride samples reached values of hardness as high as 14.2 GPa. Although high hardness values are required for implants with high wear resistance, such as hip replacements, high hardness tends to increase Young's modulus of the materials and its probability of failure.

Table 3: Vickers hardness (H_V), fracture toughness (K_{IC}) and compressive strength (σ_F).

COMPOSITION	H_V (GPa)	K_{IC} (MPa.m ^{1/2})	σ_F (MPa)
Se6	10.51 ± 0.16	6.61 ± 0.26	2,453.25 ± 111.48
Se6A	10.34 ± 0.18	6.66 ± 0.20	2,508.74 ± 115.25
Se10	9.98 ± 0.13	6.56 ± 0.26	2,440.59 ± 113.23
Se10A	9.96 ± 0.12	6.62 ± 0.19	2,461.45 ± 116.43
Se12	9.92 ± 0.10	6.66 ± 0.22	2,432.87 ± 102.84
Se12A	9.89 ± 0.18	6.64 ± 0.20	2,444.13 ± 115.84

Toxic elements possibly leached from the samples were evaluated by the viability of 3T3-NIH cells in contact with samples extracts (Figure 3) during 24 hours of incubation at 37 °C in 5 % CO₂. By Figure 3, we can verify that possible ions leached from the samples did not damage their cytotoxicity as the cells viability for all extracts is comparable that of negative control, i.e., the extracts did not impact cell mortality, a great evidence of biocompatibility of the materials.

**Figure 3:** Cell viability of control and samples extracts determined by MTS assay in 3T3-NIH cells.

The biocompatibility of the materials is the most significant property for *in vivo* applications. For this reason, many kinds of *in vitro* tests should be performed to investigate the material's potentiality for clinical devices. Here, we used the cytotoxicity test as well as the cells proliferation assay with MG63 cells. The last tests are very important for orthopedic and dental prosthesis because the ability of osteoblasts to proliferate influences the osseointegration process on the implant surface. Hence, morphology of MG63 cells on the materials surface after 7 culture days were evaluated by scanning electron micrographs (Figure 4). The micrographs show that the osteoblastic cells presented polygonal forms with a growth pattern-parallel aligned to the scratches' direction left by the final finishing. Moreover, they are covering the entire surface of all studied samples even after the small culture time, another great demonstration of the biocompatibility attributed to the microstructure, chemical compositions and surface roughness of the samples standardized by the surface finishing using a diamond grinding wheel.

The metabolic activity of the osteoblast cells on the samples surfaces was performed using MTS assay based on the absorbance of media after 7 and 21 culture days (Figure 5).

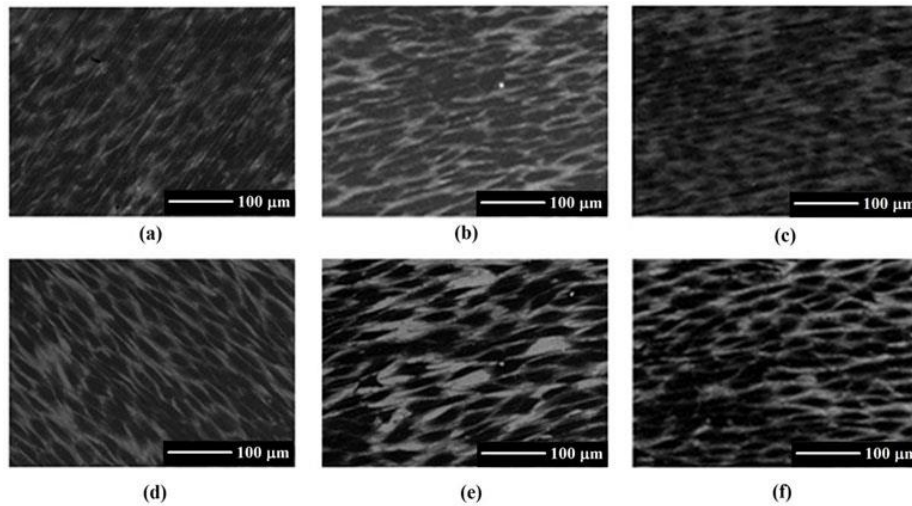


Figure 4: Scanning electron micrographs showing the MG63 cells cultured on samples during 7 days. (a) Se6; (b) Se10; (c) Se12. (d) Se6A; (e) Se10A; (f) Se12A.

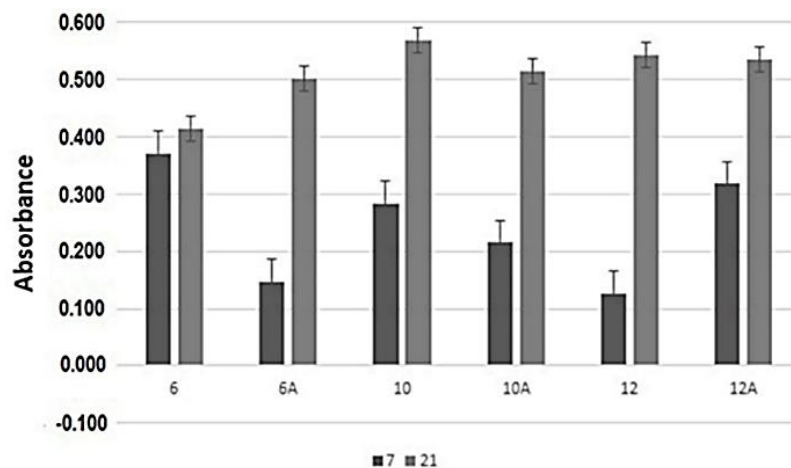


Figure 5: MTS assay at 7 and 21 days of cell culture.

From Figure 5, it is possible to note a substantial increase in cell proliferation from 7 to 21 of culture time for all samples what is another good demonstration of biocompatibility. For Se6 and Se12 samples subjected to 7 days of cell culture, it is very clear the effect of porosity on cell proliferation since they promoted higher absorbance than those ones with the same composition but also containing alumina (Se6A and Se12) and lower porosity (Table 2). For Se10 and Se10A samples, the strontium appears to have higher influence on cell proliferation than the porosity. This effect was more evident after 21 days of culture, when it is noted that the most promising sample to favor the cell growth is that with higher amount of strontium (Se10). This behavior indicates the positive impact of strontium on osteoblast proliferation, and consequently on the osseointegration process, also detected by other studies [28, 29].

Research has reported that strontium incorporations in biomaterials lead to modify their cellular response and some physico-chemical properties, such as hydrophilicity [30]. Another study about diopside ($\text{CaMgSi}_2\text{O}_6$) scaffolds without/with strontium shows that Sr-doping improves the mesenchymal stem cell adhesion and spreading [31]. Moreover, WANG *et al.* [32] reported that the presence of strontium in biomaterials increases the cell proliferation and improves the osteogenic differentiation of rabbit bone-marrow stem cells (rBMSCs). However, it is very important to point that while strontium stimulates the osteoblast proliferation and osteoclast activity [33], its high concentration in the material may also reduce both calcium concentration and mineral density in the newly bone, which makes strontium additions in biomaterials care-

fully evaluated [34].

After Se10 sample, those with the greater ability to proliferate osteoblastic cells during 21 days of culture were Se12, Se12A and Se10A, probably due to the amount of glassy phase similar to that of Se10 sample, but with lower amount of strontium. Lastly, Se6 and Se6A coded samples had the lower ability to promote cell growth also indicating the influence of glassy phase.

4. CONCLUSIONS

SiO₂, SrO and Al₂O₃ additions were appropriated to promote the liquid phase sintering of silicon nitride ceramics. Although all samples have developed elongated grains of β-Si₃N₄, high densities, relatively high values of fracture toughness and very high values of compressive strength, those with higher content of additives had the highest density and lowest hardness. In addition, the samples with high content of SrO presented the more promisor *in vitro* biological behavior expressed by the best results of cell proliferation, becoming more propitious to be used as mini-osteo-fixation systems, intervertebral fusion spacers and dental roots

5. ACKNOWLEDGMENTS

This research was funded by Fundação de Amparo à Pesquisa do Estado de São Paulo, grant number 2015/02265-7.

6. BIBLIOGRAPHY

- [1] ZIEGLER, G., HEINRICH, J., WOTTING, G., "Review relationships between processing, microstructure and properties of dense and reaction-bonded silicon nitride", *Journal of Materials Science*, v. 22, pp. 3041, 1987.
- [2] LIU, X.-J., HUANG, Z.Y., GE, Q. M., *et al.*, "Microstructure and mechanical properties of silicon nitride ceramics prepared by pressureless sintering with MgO-Al₂O₃-SiO₂ as sintering additive", *Journal of the European Ceramic Society*, v. 25, pp. 3353-3359, 2005.
- [3] WOTTING, G., ZIEGLER, G., "Influence of powder properties and processing conditions on microstructure and mechanical properties of sintered Si₃N₄", *Ceramic International*, v. 10, pp. 18-22, 1984.
- [4] SMITH, M. W., ROMANO, D. R., MC ENTIRE, B. J., *et al.*, "A single center retrospective clinical evaluation of anterior cervical discectomy and fusion comparing allograft spacers to silicon nitride cages", *Journal Spine Surg.*, v. 4, n.2, pp. 349-360, 2018.
- [5] RAMBO JR., W. M., "Treatment of lumbar discitis using silicon nitride spinal spacers: A case series and literature review", *Int J. Surg Case Rep.*, v. 43, pp. 61-68, 2018.
- [6] KERSTEN, R.F.M.R., WU, G., POURAN, B., *et al.*, "Comparison of polyetheretherketone versus silicon nitride intervertebral spinal spacers in a caprine model", *J. Biomed. Mater. Res. Part B*, v. 107 B, pp. 688-699, 2019.
- [7] LAL, S., CASELEY, E.A., HALL, R.M., *et al.*, "Biological impact of silicon nitride for orthopaedic applications: role of particle size, surface composition and donor variation", *Scientific Reports*, v. 8, pp. 1-12, 2018.
- [8] BOCK, R.M., JONES, E.N., RAY, D.A., *et al.*, "Bacteriostatic behavior of surface modulated silicon nitride in comparison to polyetheretherketone and titanium", *J. Biomed. Mater. Res. A*, v. 105A, pp. 1521-1534, 2017.
- [9] BOSCHETTO, F., ADACHI, T., HORIGUCHI, S., *et al.*, "Monitoring metabolic reactions in Staphylococcus epidermidis exposed to silicon nitride using in situ timelapse Raman spectroscopy", *Journal of Biomedical Optics*, v. 23, 056002, 2019.
- [10] PRECNEROVÁ, M., BODISOVÁ, K., FRAJKOROVÁ, F., *et al.*, "In vitro bioactivity of silicon nitride-hydroxyapatite composites", *Ceramics International*, v. 41, n.6, pp. 8100-8108, 2015.
- [11] BODISOVÁ, K., KASIAROVÁ, M., DOMANICKÁ, M., *et al.*, "Porous silicon nitride ceramics designed for bone substitute applications", *Ceramics International*, v. 39, n.7, pp. 8355-8362, 2013.
- [12] GUEDES e SILVA, C. C., HIGA, O. Z., BRESSIANI, J. C., "Cytotoxic evaluation of silicon nitride-based ceramics", *Materials Science and Engineering: C*, v. 24, n.5, pp. 643-646, 2004.

- [13] FRAJKOROVÁ, F., BODISOVÁ, K., BOHAC, M., *et al.*, “Preparation and characterisation of porous composite biomaterials based on silicon nitride and bioglass”, *Ceramics International*, v. 41 (8), pp. 9770-9778, 2015.
- [14] KUE, R., SOHRABI, A., NAGLE, D., *et al.*, “Enhanced proliferation and osteocalcin production by human osteoblast-like MG63 cells on silicon nitride ceramic discs”, *Biomaterials*, v. 20 (13), pp. 1195-1201, 1999.
- [15] HAN, W., LI, Y., CHEN, G., *et al.*, “Effect of sintering additive composition on microstructure and mechanical properties of silicon nitride”, *Materials Science and Engineering: A*, v. 700, pp. 19-24, 2017.
- [16] LIU, T., JIANG, C., GUO, W. “Effect of CeO₂ on low temperature pressureless sintering of porous Si₃N₄ ceramics”, *Journal of Rare Earths*, v. 35 (2), pp. 172-176, 2017.
- [17] GUEDES e SILVA, C. C., CARVALHO, F. M. S., BRESSIANI, J. C., “Effect of rare-earth oxides on properties of silicon nitride obtained by normal sintering and sinter-HIP”, *Journal of Rare Earths*, v. 30 (11), pp. 1177-1183, 2012.
- [18] KASJAROVÁ, M., TATARKO, P., BURIK, P., *et al.*, “Thermal shock resistance of Si₃N₄ and Si₃N₄-SiC ceramics with rare-earth oxide sintering additives”, *Journal of the European Ceramic Society*, v. 34, n.14, pp. 3301-3308, 2014.
- [19] GUEDES e SILVA, C. C., KONIG JR., B., CARBONARI, M. J., *et al.*, “Tissue response around silicon nitride implants in rabbits”, *Journal of Biomedical Materials Research. A*, v. 84A, pp. 337-343, 2008.
- [20] GUEDES e SILVA, C. C., KONIG JR., B., CARBONARI, M. J., *et al.*, “Bone growth around silicon nitride implants. An evaluation by scanning electron microscopy”, *Materials Characterization*, v. 59, pp. 1339-1341, 2008.
- [21] GUEDES e SILVA, C. C., RODAS, A. C. D., SILVA, A. C., *et al.*, “Microstructure, Mechanical Properties and in vitro Biological Behavior of Silicon Nitride Ceramics”, *Materials Research-Ibero-American Journal of Materials*, v. 21, n.6, 2018.
- [22] MAZZOCCHI, M., BELLOSI, A. “On the possibility of silicon nitride as a ceramic for structural orthopaedic implantans. Part I: Processing, microstructure, mechanical properties, cytotoxicity”, *Journal of Materials Science: Materials in Medicine*, v. 19, pp. 2881-2887, 2008.
- [23] KARLSSON, K. H., FROBERG, K., RINGBOM, T., “A structural approach to bone adhering of bioactive glasses”, *Journal Non-Crystalline Solids*, v. 72, pp. 69-72, 1989.
- [24] ANSTIS, G. R., CHANTIKUL, P., LAWN, B. R., *et al.*, “A critical evaluation of indentation techniques for measuring fracture toughness: I, Direct crack measurements”, *Journal American Ceramics Society*, v. 64, pp. 533-554, 1981.
- [25] MATOVIC, B., RIXECKER, G., ALDINGER, F., “Pressureless sintering of silicon nitride with lithia and yttria”, *Journal of the European Ceramic Society*, v. 24, pp. 3395-3398, 2004.
- [26] DAS, M., BHIMANI, K., BALLA, V.K., “In vitro tribological and biocompatibility evaluation of sintered silicon nitride”, *Materials Letters*, v. 212, pp.130-133, 2018.
- [27] Liu, X.J., HUANG, Z.Y., GE, Q.M., *et al.*, “Microstructure and mechanical properties of silicon nitride ceramics prepared by pressureless sintering with MgO-Al₂O₃-SiO₂ as sintering additive” *Journal of the European Ceramic Society*, v. 25, p.p. 3353-3359, 2005.
- [28] MARIE, P. J., AMMANN, P., BOIVIN, G., REY, C., “Mechanisms of action and therapeutic potential of strontium in bone”, *Calcified Tissue International*, v. 69, pp. 121-129, 2001.
- [29] BONNELLYE, E., CHABADEL, A., SALTEL, F., *et al.*, “Dual effect of strontium ranelate: Stimulation of osteoblast differentiation and inhibition of osteoclast formation and resorption in vitro”, *Bone*, v. 42, pp. 129-138, 2008.
- [30] ROMERO-GAVILÁN, F., ARAÚJO-GOMES, N., GARCIA-ARNÁEZ, I., *et al.*, “Strontium incorporation into sol-gel biomaterial on their protein adsorption and cell interactions”, *Colloidals and Surfaces B: Biointerfaces*, v. 174, pp. 9-16, 2019.
- [31] SHAHROUZIFAR, M.R., SALAHINEJAD, E., “Strontium doping into diopside tissue engineering scaffolds”, *Ceram. Int.*, v. 45, pp. 10176-10181, 2019.
- [32] WANG, S., LIU, L., ZHOU, X., *et al.*, “Effect of strontium-containing on the properties of Mg-doped wollastonite bioceramic scaffolds”, *Biomedical Engineering Online*, v. 18, pp. 1-14, 2019.

- [33] XIN, Y. C., JIANG, J., HUO, K. F., *et al.*, “Bioactive SrTiO₃ nanotube arrays: strontium delivery platform on Ti-based osteoporotic bone implants”, *ACS Nano*, v. 3, pp. 3228-3234, 2009.
- [34] PORS NIELSEN, S. “The biological role of strontium”, *Bone*, v. 35, pp. 583-588, 2004.

ORCID

Sergio Ferreira do Nascimento

<https://orcid.org/0000-0001-8762-4956>

Andrea Cecilia Dorion Rodas

<https://orcid.org/0000-0001-9920-6882>

Flávio Machado de Souza Carvalho

<https://orcid.org/0000-0002-0640-014X>

Olga Zazuco Higa

<https://orcid.org/0000-0002-0883-745X>

Cecilia Chaves Guedes e Silva

<https://orcid.org/0000-0002-3839-0839>